J Mater Sci (2012) 47:7117–7123
DOI 10.1007/s10853-012-6408-0

SINTERING 2011

Microstructures and mechanical properties of Mg–Zn–Y alloy consolidated from gas-atomized powders using high-pressure torsion

Eun Yoo Yoon · Dong Jun Lee · Taek-Soo Kim · Hong Jun Chae · P. Jenei · Jeno Gubicza · Tamas Ungár · Milos Janecek · Jitka Vratna · Sunghak Lee · Hyoung Seop Kim

Received: 29 September 2011 / Accepted: 9 March 2012 / Published online: 22 March 2012

Abstract In this paper, rapid solidified $Mg_{95}Zn_{4.3}Y_{0.7}$ (at.%) alloy powders produced by an inert gas atomizer were consolidated using a severe plastic deformation technique of high pressure torsion (HPT) at room temperature and 373 K. The behavior of powder consolidation, matrix microstructural evolution, and mechanical properties of the powders and compacts were investigated using X-ray diffraction, scanning electron microscopy, transmission electron microscopy, microhardness, and tensile testing. As the HPT processing temperature increases, the powders are more plastically deformed due to decreased deformation resistance, grain boundaries are more in equilibrium, powder bonding is enhanced due to increased interparticle diffusion, hence, tensile ductility and strength increases. On the other hand, hardness decreases with the increased processing temperature, due to less dislocation density.

E. Y. Yoon · D. J. Lee · S. Lee · H. S. Kim (✉)
Department of Materials Science and Engineering, POSTECH, Pohang 790-784, Korea
e-mail: hskim@postech.ac.kr

T.-S. Kim · H. J. Chae
Department of Rare Metals, Korea Institute of Industrial Technology, Incheon 406-130, Korea

P. Jenei · J. Gubicza · T. Ungár
Department of Materials Physics, Eötvös Loránd University, Budapest, P.O.B. 32, 1518, Hungary

M. Janecek · J. Vratna
Department of Metal Physics, Charles University, 121 16 Prague 2, Czech Republic

Introduction

Recently, Mg alloys have been attracting a considerable amount attention due to their great potential for structural and functional applications, their low density, and their abundance in earth's crust [1–4]. However, their low strength, ductility, and corrosion resistance have limited their extension to further engineering applications. There have been several approaches to improve the poor strength and ductility of Mg alloys. A typical attempt to improve the strength of the Mg alloys is through alloy design and development with the addition of rare earth elements [3–10]. For example, Mg–Zn–Y alloys present enhanced strength and hardness, a low friction coefficient, and low interfacial energy at both room temperature and elevated temperatures, as a result of a homogeneous distribution of metastable icosahedral phase (I-phase) in the Mg phase matrix [11, 12].

While conventional routes of casting and solidification are limited in terms of microstructure control, e.g., in terms of grain refinement or inhibiting grain coarsening, the design of alloys via powder metallurgy (PM) with rapid solidification (RS), such as that gained by melt spinning or atomization, has become a general method for enhancing the mechanical properties by grain refinement or by amorphous phase formation [13]. RS-processed Mg and Mg alloy powders are challenging materials when used to manufacture high-performance structural engineering parts. A recent advance in the RS-PM technique is regarded as a promising alternative in overcoming the drawback of cast alloys: the low production and complicated procedure of melt spinning [14]. However, the RS-PM processing of Mg alloys has not progressed much due to dangers related to the processing of unstable powders. An alternative approach is powder ball milling [15]. Recently, some

reports on RS-PM processed Mg alloys represented remarkably high strength of approximately 600 MPa, although the processing was conducted using a closed system involving high vacuum atomization and extrusion to prevent surface oxidation and contamination. However, closed atomization and extrusion system is expensive; thus, more economic methods for controlling and treating surface oxidation on Mg alloy powders are needed [16, 17].

A second strategy with which the strength of Mg alloys can be enhanced is by grain refinement. Among the various methods of grain refinement, plastic deformation and rapid solidification processes have been frequently used [18–21]. In particular, as a recently emerged technique, severe plastic deformation (SPD) processing is a new method of manufacturing bulk metallic materials having ultrafine-grained (UFG) or nanostructured materials [22–24] by imposing intensive plastic strain on the materials. Among the various SPD methods, high-pressure torsion (HPT) is known as the most effective SPD process for grain refinement because a much larger amount of strain can be imposed with relative ease compared to any other SPD processes, such as the well-known equal channel angular pressing and accumulative roll bonding process. In the HPT process, the samples are placed between two anvils, subjected to a high applied hydrostatic pressure greater than 1 GPa and simultaneous torsion-strained [25, 26], as shown in Fig. 1. The HPT process has been applied mostly in the grain refinement of bulk solid materials, but it is sufficient for the consolidation of metastable powders, e.g., amorphous or nano-scale powders, to densify materials fully [27, 28], as the processing temperature is lower than any other powder sintering or consolidation temperatures.

The present authors envisage that the HPT process would be effective in the consolidation of $Mg_{95}Zn_{4.3}Y_{0.7}$ alloy powders with the enhanced mechanical properties using the combined effect of a low consolidation temperature and a large amount of applied strain. In this paper, we report the microstructure and mechanical properties of flammable $Mg_{95}Zn_{4.3}Y_{0.7}$ alloy powders prepared via gas atomization, and the variation of microstructure and mechanical properties of an $Mg_{95}Zn_{4.3}Y_{0.7}$ alloy disk consolidated by HPT. The HPT results are compared to those from an extrusion process of the same powders.

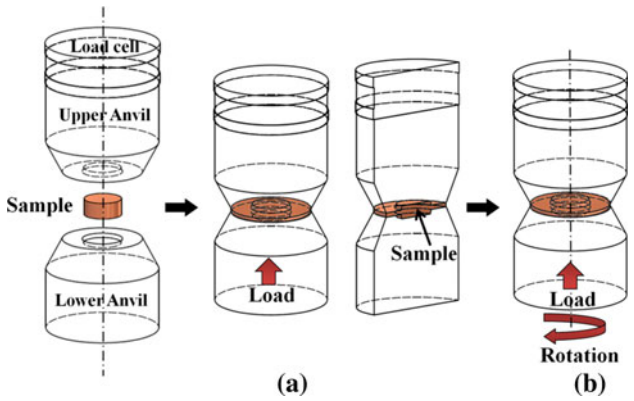

Fig. 1 Schematic of the HPT device showing the set-up, **a** compression stage and **b** compression-torsion conditions

Experimental procedure

Gas-atomization of $Mg_{95}Zn_{4.3}Y_{0.7}$ alloy

The $Mg_{95}Zn_{4.3}Y_{0.7}$ alloy powders were fabricated using a high-pressure gas-atomizing process consisting of a boron nitride melt-delivery nozzle 5 mm in diameter and an annular Ar gas nozzle. The melt flow rate, estimated from the operating time and the weight of the atomized melt, was approximately 1.0 kg/min, while the applied gas pressure was 5 MPa. The surface oxide layers of the powders were artificially introduced by controlling the chamber atmosphere to prevent an explosion of the flammable Mg alloy powders. The microstructure of the atomized powder was characterized by scanning electron microscopy (FESEM: JEOL JSM 6330F) at 15 kV.

High-pressure torsion

Due to the surface oxide layers and possible contaminants in the atomized powders, incomplete powder consolidation can occur in conventional powder metallurgy routes, such as extrusion, sintering, or forging. To improve interparticle bonding, a mechanical method and a thermal method can be used. The HPT process as the former method involves breaking the surface oxides, exposing the virgin atoms covered by oxide films, moving the virgin atoms close to each other, and finally achieving metallic bonding.

HPT processing was conducted at room temperature and at 373 K to investigate the effects of the processing temperature on the powder consolidation and mechanical properties. For the elevated-temperature processing condition, the upper and lower anvils were initially heated up without the sample in place until the desired temperature was reached. Afterward, the anvils were separated and a pre-compacted Mg alloy in the shape of a disk was placed in a circular groove at the center of the lower anvil, as illustrated in Fig. 1. Hydraulic pressure of 2.5 GPa was applied to the lower anvil loaded with the pre-compacted Mg alloy disk, by lifting it to the operating position. The upper die remained at a fixed position during and after the compression stage, while the lower die rotates up to 10 revolutions at a constant speed of 1 rpm to apply shear strain to the sample. The applied pressure of 2.5 GPa was kept constant during the compression and torsioning stages.

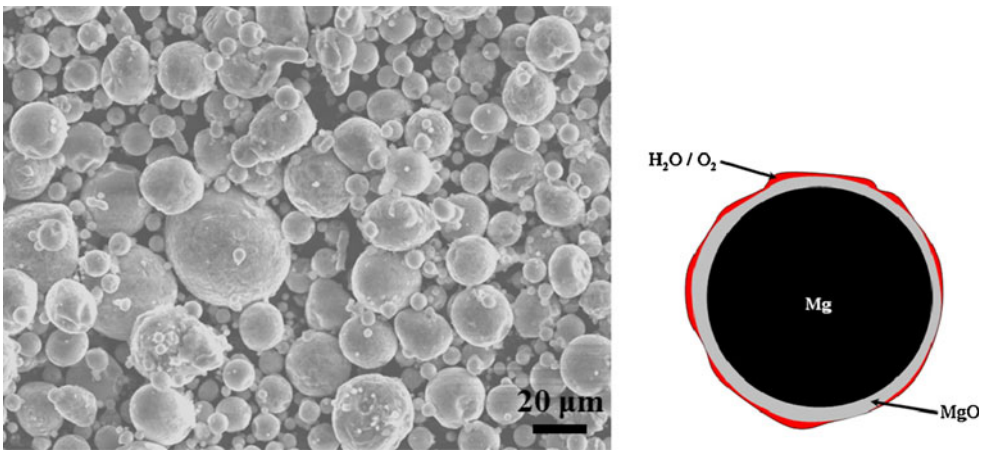

Fig. 2 Morphology of a typical spherical $MgZn_{4.3}Y_{0.7}$ alloy powder formed by gas atomization as observed by FESEM and a schematic of the surface oxide layers in $MgZn_{4.3}Y_{0.7}$ alloy powders

The final geometry of the HPT-processed sample was 20 mm in diameter and 0.8 mm in height.

Characterization

After the HPT process, the surfaces of the disks were mechanically polished to a mirror-like finish for the FE-SEM observations and microhardness measurements. The measurements were taken to determine the Vickers microhardness Hv at selected positions across the diameter of each disk with incremental steps of 0.5 mm estimated using a Future-Tech FM-700 tester. The applied load and dwell time were 100 g and 20 s, respectively. For tensile testing, two dog-bone-type specimens were cut from a HPT disk using a wire cutting machine at a position 2 mm away from the center. In the tensile samples, the gauge length was 2.2 mm and width was 1.5 mm. The tensile tests were performed at room temperature with an initial strain rate of 1.0×10^{-3} s^{-1}. During the tensile tests, precise strains were measured by a vision strain gauge system (ARAMIS 5M) capable of detecting the three-dimensional coordinates of the deforming surface on the basis of digital image processing.

The microstructure of the solid disks produced by the HPT process was examined by transmission electron microscopy (TEM: JEOL 2000FX) operating at 200 kV. Thin foils for TEM were prepared by mechanical grinding followed by ion-milling using PIPS Gatan at 4 kV.

Results and discussion

The gas-atomized $Mg_{95}Zn_{4.3}Y_{0.7}$ alloy powders as measured by a conventional mechanical sieving technique shows a spectrum 32–150 μm in diameter. The shape of the atomized powders is almost spherical, as shown in Fig. 2. Coarse particles are globular with slightly rough surfaces, compared to the fine spherical particles with smooth surfaces. Small satellite particles [29] exit on the surface of large particles, which exhibit dendritic surface reliefs. In order to inhibit the explosive reaction of Mg or Mg alloys with oxygen, we intentionally formed Mg oxide films on the surface of the powders, as shown in the schematic of the Mg alloy powder (Fig. 2). In order to measure the depth of the oxide layer, the atomized powders were etched from the surfaces using an Ar gas. Considering an error range of 10 % in the Auger electron spectroscopy detection process, the thickness of the Mg oxide was determined to be approximately 48 nm [30].

Figure 3 represents the microstructures of the disks processed by HPT at room temperature and 373 K as observed using FESEM. This figure shows the center, middle (5 mm from the center), and edge (9 mm from the center) regions. In Fig. 3a, b, and d, show traces of many undeformed powders. The HPT disks processed at room temperature, shown in Fig. 4a, b, and d, show traces of many undeformed powders. The undeformed powders arose due to their low applied strain and high deformation resistance at the low applied strain in the center and middle regions. Hence, the amount of the undeformed powder trace decreases with (i) an increase in the distance from the center, as the torsional strain increases linearly with the distance from the center, and (ii) an increase in the HPT processing temperature, as the deformation resistance decreases with an increase in the temperature. The small amount of deformation of the powders processed at room temperature was modified by increasing the HPT processing temperature, as shown in Fig. 3d–f. However, many powders processed at 373 K remain undeformed in the center region, as shown in Fig. 3d, due to the lower applied strain by HPT than in the middle and edge regions.

At a HPT of 373 K, although the temperature was low compared to those in the other powder consolidation processes with the same composition powders [20, 30, 31], most of the powders were plastically deformed except in the center region, as shown in Fig. 3d. It is reasonable to

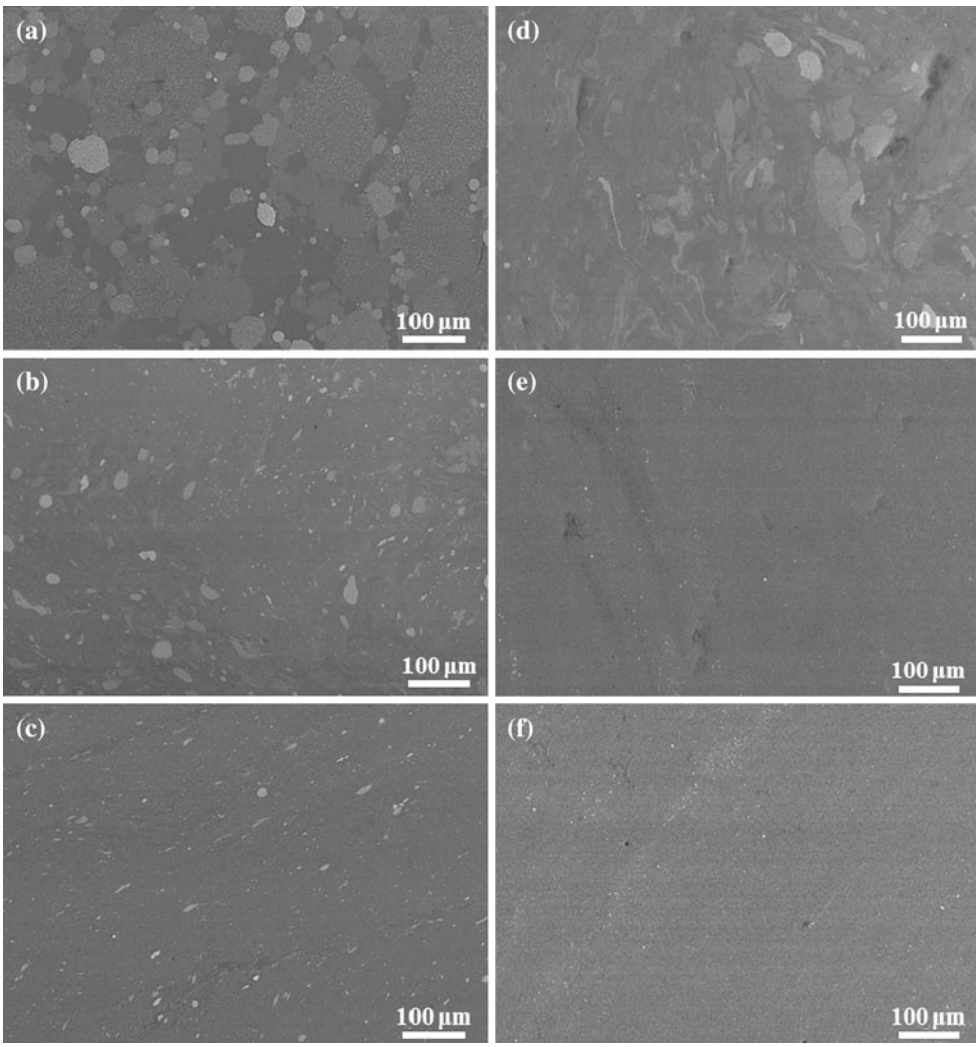

Fig. 3 FESEM micrographs in the HPT-processed disks processed at two different processing temperatures: **a** center, **b** middle, and **c** edge regions of the disk processed at room temperature, and **d** center, **e** middle, and **f** edge regions of the disk processed at 373 K

conclude, therefore, that the increased uniformity near the edge of the disk compared to the middle and center regions is due to the large shear and hydrostatic strains that developed at the edge region, leading to straightforward powder deformation and consolidation. Moreover, it is clear that an elevated temperature helps to consolidate the Mg alloy powders. Examining Fig. 3b versus 3e and 3c versus 3f with the same shear strain received, it is clear that an increased processing temperature is effective for the homogeneous deformation of $Mg_{95}Zn_{4.3}Y_{0.7}$ alloy powders. At a higher temperature, powders are more easily deformed and the degree of powder consolidation is enhanced due to the combined effect of faster atomic diffusion and lower deformation resistance. In addition, the atoms on the powder surface diffuse through the inter-powder region after breaking the hard oxide layers as shown in Fig. 2. The oxide layer formed on the Mg alloy powder surfaces has a composition of MgO, which is slightly more porous, and it has a melting point of 3,073 K [32]. The oxide layers are generally formed during atomization and can be broken and spread in the Mg matrix in the temperature range of 373–573 K [30, 31, 33].

The TEM analysis in Fig. 5 represents the temperature and stain effects on the consolidation of the HPT-processed Mg alloy disks. Bright- and dark-field images are shown in Fig. 4a–c of the room-temperature sample and in Fig. 4b–f of the sample processed at 373 K at three regions of the center (Fig. 4a, d), middle (Fig. 4b, e), and edge (Fig. 4c, f). The center region of the disk processed at room temperature shows a heavily deformed structure with high density of tangled dislocations. In some areas subgrains were also found. In the middle (Fig. 4b) of the specimen and in zones near specimen edge (Fig. 4c), which were subjected to higher strain, grain formation occurred. Grains with many dislocations were observed in the microstructure. The average grain size, determined from a series of dark-field images, in the middle of the specimen varied between 200 and 300 nm, while in the edge more developed grain fragmentation occurred resulting in the grain size in the range of 100–150 nm.

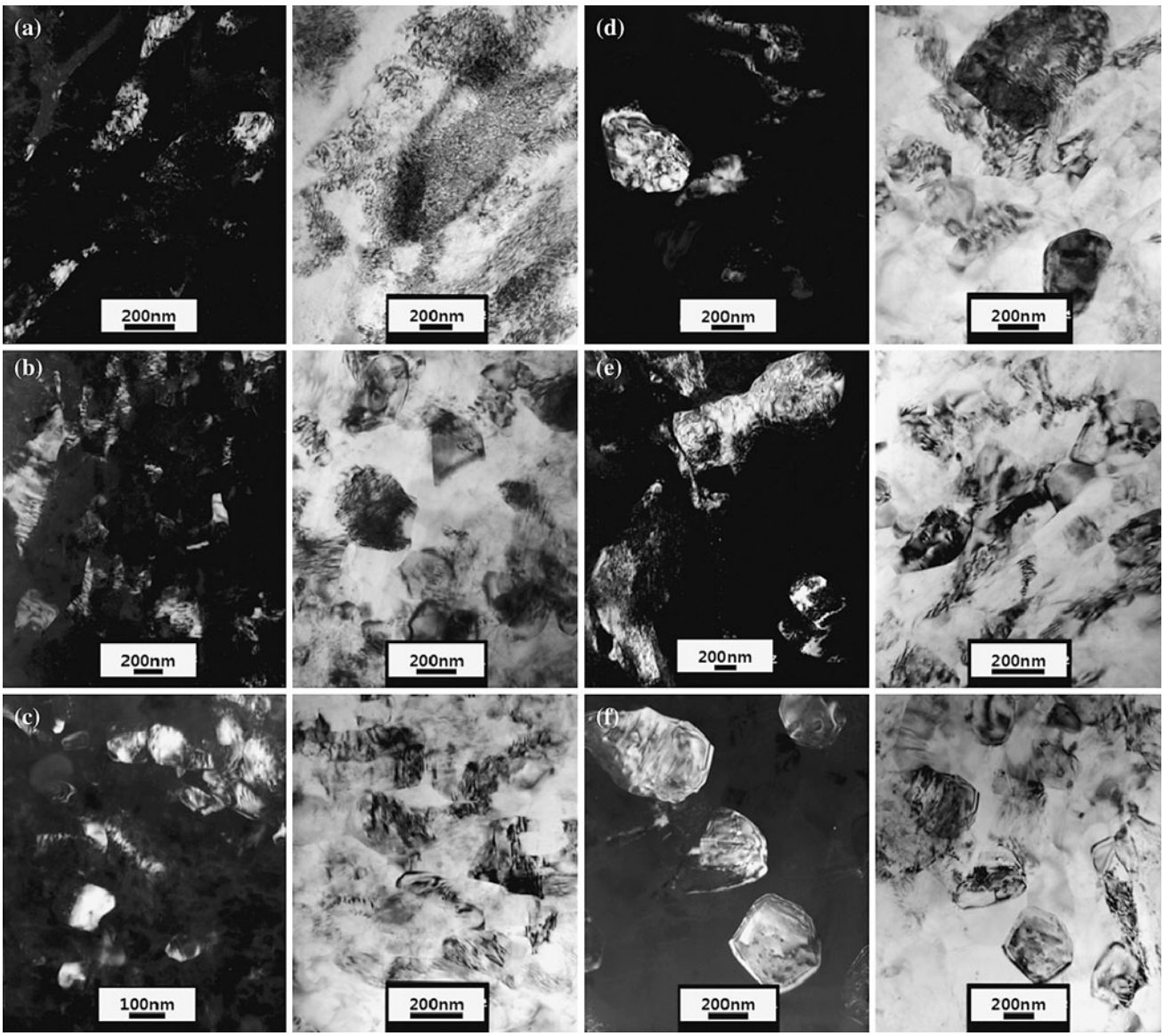

Fig. 4 Microstructure recorded by TEM of dark-field and bright-field images after HPT processing at two different temperatures: **a** center, **b** middle, and **c** edge regions of the disk processed at room temperature and **d** center, **e** middle, and **f** edge regions of the disk processed at 373 K

At higher temperature ($T = 373$ K) the microstructure evolution with strain is qualitatively similar to that at RT. However, the detail inspection of TEM micrographs reveals some differences. In the specimen center subgrains/grains of the average size of 500 nm with many dislocations and non-equilibrium grain boundaries with diffuse fuzzy contrast [22] are visible (Fig. 4d). At higher strains (in the middle and in particular near the edge of the specimen) partial recrystallization has already occurred resulting in the formation of new grains with very few dislocations separated by high angle grain boundaries with typical thickness fringe contrast. This is clearly seen especially in the Fig. 4f, which represents the typical microstructure in zones near the edge of the HPT disk at 373 K.

The Vickers microhardness of the Mg alloy disks are plotted from the disk center to the edge in Fig. 5, showing the increased hardness from the center to the edge. The hardness of the extrudate is also included. The maximum hardness reached 170 Hv at the edge of the room-temperature processed disk, which is much higher than those at the center and middle regions of the HPT disks and in the extruded $Mg_{95}Zn_{4.3}Y_{0.7}$ alloy bars with extrusion ratios of 10:1, 15:1, and 20:1 [31]. This very high hardness in the HPT samples compared to the extrudate is due to the fine grain size and high dislocation density caused by the HPT

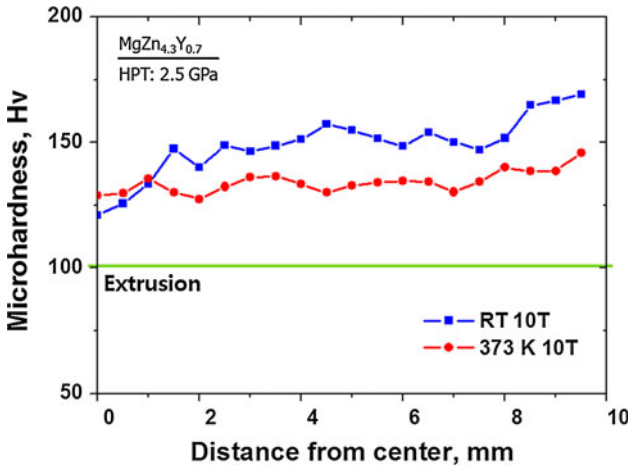

Fig. 5 Average value of the Vickers microhardness, Hv, plotted against the distance from the center of the disk after processing by HPT at two different temperatures at an applied pressure of 2.5 GPa and a comparable extrusion bar hardness value

processing at a high level of shear strain with well-dispersed oxide. The center region of the room-temperature disk shows lower hardness values due to the lower consolidation of the powders, as shown in Fig. 3a. Nevertheless, across the diameter of the disks in the center regions, the room-temperature sample shows higher hardness values due to the combined effect of a finer grain size and a higher dislocation density, as shown in Fig. 4a and d. It is interesting that the microstructural features, i.e., grain size and dislocation density, are more important than the interparticle bonding for hardness.

Tensile stress–strain curves of the HPT-processed $Mg_{95}Zn_{4.3}Y_{0.7}$ alloy with two different processing temperatures are presented in Fig. 6. At room temperature and at 373 K, the ultimate tensile strength (UTS) values are approximately 414 and 447 MPa, respectively. The failure

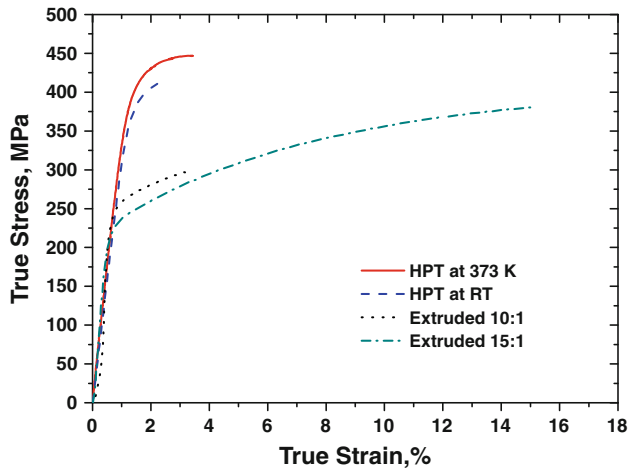

Fig. 6 Tensile curves of HPT-processed Mg alloy disks processed at two different temperatures and a comparable extruded bar

elongation was enhanced from 2.5 to 3.5 % with an increase in the processing temperature. The improvement in both the stress level and elongation in the disks processed at 373 K can be explained by the microstructural homogeneity and the good powder bonding shown in Fig. 3e, i.e, defects by the microstructural inhomogeneity and imperfect powder bonding probably are more in the room-temperature HPT specimen than in the 373 K HPT specimen. It should be noted that hardness and compressive strength are less sensitive to the defect density. Therefore, the room-temperature HPT specimen is stronger in compression due to more dislocations and weaker in tension due to more imperfect debonding regions than the 373 K HPT specimen. The tensile strength of the sample processed at 373 K of 447 MPa was higher than not only 370 MPa by hot rolling but also 380 MPa in extrudates of the same composition, while the elongation 3.5 % is lower than the value of 17.2 % via hot rolling and 16 % by extrusion [6, 31]. To sum up, HPT can increase the strength of metallic materials by enhancing grain refinement and dislocation density, and achieve powder consolidation through the effect of high shear and hydrostatic stresses. Increasing HPT processing temperature promotes a homogeneous and almost completely deformed microstructure. Furthermore, better mechanical properties and better consolidation can be expected by increasing the number of HPT revolutions in an effort to impose greater amount of shear strain.

Conclusions

In this paper, the following conclusions from the experimental investigations of the $Mg_{95}Zn_{4.3}Y_{0.7}$ alloy powder processed by HPT were drawn.

1. $Mg_{95}Zn_{4.3}Y_{0.7}$ alloy powders atomized using an Ar gas atomizer presented an almost spherical morphology, and could be consolidated by the HPT process at two temperatures.
2. Due to the low shear strain in the torsion theory, particles in the center region remain pancake-shaped even after HPT at 373 K. Near the edge of the HPT-processed disk, homogeneous and highly deformed microstructures were obtained, representing better properties with almost full consolidation.
3. The consolidated Mg alloy disks showed ultrafine grained structures and many dislocations which explained the superior hardness value (170 Hv) compared to the extruded bar (90–92 Hv).
4. The elevated temperature HPT process achieved ultrafine-grained microstructures with more equilibrium grain boundaries and better deformed structures.

Therefore, the tensile strength increased from 404 to 433 MPa, and the elongation also increased from 2.5 to 3.5 %, with an increase in the processing temperature from room temperature to 373 K.

Acknowledgements This study was supported by the National Research Foundation of Korea (NRF) grant funded by the Korea government (MEST) (No. 2010-0026981).

References

1. http://en.wikipedia.org/wiki/Magnesium. Accessed 17 March 2012
2. Estrin Y, Yi SB, Brokmeier HG, Zuberova Z, Yoon SC, Kim HS, Hellmig RJ (2008) Int J Mater Res 99:50
3. Kim WJ, Hong SI, Lee KH (2010) Metal Mater Inter 16:171
4. Kim DH, Lim HK, Kim YK, Kyeong JS, Kim WT, Kim DH (2011) Metal Mater Inter 17:383
5. Suzuki M, Kimura T, Koike J, Maruyama K (2003) Scripta Mater 48:997
6. Kim SH, Kim DH, Kim NJ (1997) Mater Sci Eng A 226–228:1030
7. Shin B, Kim Y, Bae D (2008) J Korean Inst Met Mater 46:1
8. Shin B, Yoon S, Ha C, Yun S, Bae D (2010) Korean J Met Mater 48:116
9. Kang MG, So TI, Jung HC, Shin KS (2011) Korean J Met Mater 49:686
10. Lee BD, Baek UH, Jang KS, Han JW, Son HT (2011) Korean J Met Mater 49:440
11. Bae DH, Kim SH, Kim DH, Kim WT (2002) Acta Mater 50:2343
12. Kim DH, Kim YK, Kim WT, Kim DH (2011) Korean J Met Mater 49:145
13. Cai J, Ma GC, Liu Z, Zhang HF, Hu ZQ (2006) J Alloy Compd 422:92
14. Nishida M, Kawamura Y, Yamamoto T (2004) Mater Sci Eng A 375–377:1217
15. Crivello J-C, Nobuki T, Kuji T (2007) Intermetallics 15:1432
16. Kawamura Y, Hayashi K, Inoue A, Masumoto T (2001) Mater Trans 42:1172
17. Inoue A, Kawamura Y, Matsushita M, Hayashi K, Koike J (2001) J Mater Res 16:1894
18. Yoon SC, Bok CH, Seo MH, Hong SJ, Kim HS (2008) J Korean Powder Metal Inst 15:31
19. Kim HS (2002) Mater Sci Eng A 328:317
20. Kim TS, Chae HJ, Lee JK, Jung HG, Bae JC (2007) Mater Sci Forum 534:793
21. Kim HS, Estrin Y, Bush MB (2000) Acta Mater 48:493
22. Valiev RZ, Islamgaliev RK, Alexandrov IV (2000) Prog Mater Sci 45:103
23. Valiev RZ, Estrin Y, Horita Z, Langdon TG, Zehetbauer MJ, Zhu YT (2006) JOM 58:33
24. Kim HS, Seo MH, Hong SI (2000) Mater Sci Eng A 291:86
25. Zhilyaev AP, Langdon TG (2008) Prog Mater Sci 53:893
26. Song YP, Yoon EY, Lee DJ, Lee JW, Kim HS (2011) Mater Sci Eng A 528:4840
27. Stolyarov VV, Zhu YT, Lowe TC, Islamgaliev RK, Valiev RZ (2000) Mater Sci Eng A 282:78
28. Alexandrov IV, Zhang K, Kilmametov AR, Lu K, Valiev RZ (1997) Mater Sci Eng A 234–236:331
29. Hong SJ, Kim T-S, Kim HS, Kim WT, Chun BS (1999) Mater Sci Eng A 271:469
30. Kim T-S, Chae HJ (2008) Rev Adv Mater Sci 18:769
31. Kim T-S (2010) J Alloys Compd 504S:S496
32. Amaral LF, Oliveira IR, Salomao R, Frollini E, Pandolfelli VC (2010) Ceram Int 36:1047
33. Chae HJ, Kim YD, Kim T-S (2011) J Alloys Compd 509S:S250